Supersymmetric minimal $U(1)_X$ model at the TeV scale with right-handed Majorana neutrino dark matter

Nobuchika Okada[1] and Desmond Villalba[2]

[1]*Department of Physics and Astronomy, The University of Alabama, Tuscaloosa, Alabama 35487, USA*
[2]*Department of Chemistry and Physics, University of Mary Washington,
Fredericksburg, Virginia 22401, USA*

We propose a supersymmetric extension of the minimal $U(1)_X$ model, along with a new Z_2 parity. One of the salient features of this model relates to how both the $U(1)_X$ gauge symmetry and R parity are broken radiatively at the TeV scale by the vacuum expectation value of a Z_2-even right-handed sneutrino. By assigning one right-handed neutrino Z_2-odd parity, it can remain a viable dark matter (DM) candidate, despite R parity being broken. Furthermore, the DM relic abundance receives an enhanced annihilation cross section due to the $U(1)_X$ gauge boson (Z') resonance and is in agreement with the current observations. We have also found a complementarity that exists between the observed DM relic abundance and search results for the Z' boson resonance at the Large Hadron Collider, which further constrains the parameter space of our $U(1)_X$ model. Finally, we consider a $SU(5) \times U(1)_x$ grand unified theory extension and investigate the complementarities mentioned previously.

I. INTRODUCTION

The minimal supersymmetric (SUSY) extension of the Standard Model (MSSM) is one of the prime candidates for physics beyond the Standard Model, which naturally solves several problems in the SM, in particular, the gauge hierarchy problem. In addition, a candidate for the cold dark matter, which is missing in the SM, is also naturally incorporated in the MSSM. The search for SUSY is one of the major directives of the Large Hadron Collider (LHC), which is operating at unprecedented luminosities, and is collecting data very rapidly.

Remarkably, the MSSM can solve the gauge hierarchy problem and the dark matter problem. It is able to achieve the feat by mere virtue of it being supersymmetric. However, it is clear that the SUSY extension is not enough to solve the aforementioned problems in addition to explaining neutrino phenomena. Both the observed solar and atmospheric neutrino oscillations, as well as long and short baseline experiments have established nonzero neutrino masses and mixings between different neutrino flavors [1]. Unlike the quark sector, the scale of neutrino masses is very small and the different flavors are largely mixed. To make the MSSM a more viable description of

nature, we have no choice but to extend it, so that it incorporates neutrino masses and flavor mixings. The well-known seesaw extension [2] has garnered much support since it not only accounts for the neutrino mass but also explains the smallness of the mass in a more "natural" way. Depending on the seesaw scale (typically the scale of right-handed neutrinos) being, for example, from 1 TeV to 10^{14} GeV, the scale of the neutrino Dirac mass varies from 1 MeV (the electron mass scale) to 100 GeV (the top quark mass scale).

As the $B - L$ (baryon number minus lepton number) is an anomaly-free global symmetry in the SM, it can be easily gauged. The minimal $B - L$ model is the simplest gauged $B - L$ extension of the SM [3], where three generations of right-handed neutrinos and a Higgs field with two units of the $B - L$ charge are introduced. The presence of the three right-handed neutrinos is essential for canceling the gauge and gravitational anomalies. The general extension of the $B - L$ to the $U(1)_X$ model has been carried out [4], where the particle contents are the same except for the $U(1)_X$ charge assignment [5]. The $U(1)_X$ charge for a field is defined as a linear combination of $B - L$ and the hypercharge, $Q_x = Y x_H + Q_{B-L}$, where x_H is a real parameter. In the limit of $x_H \to 0$, the MSSM $U(1)_{B-L}$ model is attained. As in the $B - L$ case, it has been shown that the $U(1)_X$ model is free of anomalies [6].

While the energy scale of the $U(1)_X$ gauge symmetry breaking is subject to some phenomenological constraints, the energy breaking scale is weakly constrained. Interestingly, through considerations of dark matter and collider

physics, we have found that only a small window in the parameter region of a few TeV is allowed for the $U(1)_X$ model to remain viable. If this is the case, we can expect that all new particles in the model, the $U(1)_X$ gauge boson Z', the $U(1)_X$ Higgs boson, and the right-handed neutrinos appear at the TeV scale, which can be discovered at the LHC [7].

In this paper, we investigate supersymmetric extension of the minimal $U(1)_X$ model. It has been previously shown [8] that an analogous mechanism to radiative electroweak symmetry breaking in the MSSM exists for the case where the $U(1)_{B-L}$ symmetry is radiatively broken by the interplay between large Majorana Yukawa couplings of right-handed neutrinos and the soft SUSY breaking masses. Employing the same mechanism naturally places the $U(1)_X$ symmetry breaking scale at the TeV scale.

Despite this remarkable feature of the SUSY minimal $U(1)_{B-L}$ and our $U(1)_X$ model, a more thorough analysis [9] indicated that most of the $U(1)_{B-L}$ symmetry breaking parameter space is occupied by nonzero vacuum expectation values (VEVs) from right-handed sneutrinos. Therefore, the most likely scenario in the SUSY minimal $U(1)_X$ model with the radiative $U(1)_X$ symmetry breaking is that R parity is violated in the vacuum. This means that the lightest superpartner (LSP) neutralino, which is the conventional dark matter candidate in SUSY models, becomes unstable and no longer remains a viable dark matter candidate. As discussed in [10], even though R parity is broken, an unstable gravitino if it is the LSP has a lifetime longer than the age of the Universe and can still be the dark matter candidate.

A cogent framework for dark matter has been discussed previously in the context of the (non-SUSY) minimal $B - L$ model [11] and a $B - L$ MSSM [12], where a new Z_2 parity was introduced and one right-handed neutrino was assigned odd-Z_2 parity while the other fields were assigned even Z_2. Calculation of the relic abundance of the Z_2-odd right-handed neutrino showed that it could account for the observed relic abundance and therefore the dark matter in our Universe. We mention this to emphasize that we are not introducing any new particles in the current model.

In this paper, we apply the same idea to the SUSY generalization of the minimal $U(1)_X$ model with the radiative $U(1)_X$ symmetry breaking and investigate the resulting phenomenology. What we discovered is that the $U(1)_X$ gauge symmetry and R parity are both broken at the TeV scale by the nonzero VEV of a Z_2-even right-handed sneutrino, for suitable regions of parameter space. Even in the presence of R-parity violation, the Z_2 parity is still exact and the stability of the Z_2-odd right-handed neutrino is guaranteed. Therefore, the Z_2-odd right-handed neutrino appears to be a natural, stable dark matter candidate. We calculated the relic abundance of the Z_2-odd right-handed neutrino and found that the resultant relic abundance was in agreement with observations.

This paper is organized as follows. In the next section, we define the SUSY minimal $U(1)_X$ model with Z_2 parity and introduce superpotential and soft SUSY breaking terms relevant for our discussion. In Sec. III, we perform a numerical analysis of the renormalization group equation (RGE) evolution of the soft SUSY breaking masses of the right-handed sneutrinos and $U(1)_X$ Higgs fields and show that the $U(1)_X$ gauge symmetry is radiatively broken at the TeV scale. It will be shown that one Z_2-even right-handed sneutrino develops a VEV, and hence R parity is also radiatively broken. In Sec. IV, we calculate the relic abundance of the right-handed neutrino and identify the parameter region consistent with the observed dark matter relic abundance. We also discuss phenomenological constraints of the model in Sec. V. In Sec. VI, we extend the model to the $SU(5) \times U(1)_X$ gauge group and discuss SM gauge unification. The last section is devoted to conclusions and discussions.

II. SUPERSYMMETRIC MINIMAL $U(1)_X$ MODEL WITH Z_2 PARITY

The minimal $U(1)_X$ extended SM is based on the gauge group $SU(3)_c \times SU(2)_L \times U(1)_Y \times U(1)_X$ with three right-handed neutrinos and one Higgs scalar field with $U(1)_X$ charge 2, which is a singlet under the SM gauge group. The $U(1)_X$ charges are defined as a linear combination of $B - L$ and the hypercharge, $Q_x = Y x_H + Q_{B-L}$, where x_H is a real parameter. As far as the motivation to introduce three generations of right-handed neutrinos (N_i^c) is concerned, the introduction of the three generations of right-handed neutrinos is in no way *ad hoc*; on the contrary, once we gauge $U(1)_X$, their introduction is forced upon us by the requirement of the gauge and gravitational anomaly cancellations. The SM singlet scalar works to break the $U(1)_X$ gauge symmetry by its VEV and, at the same time, generates Majorana masses for right-handed neutrinos, which then participate in the seesaw mechanism.

It is easy to supersymmetrize this model and the particle contents are listed in Table I.[1] The gauge invariant superpotential relevant for our discussion is given by

$$W_{BL} = \sum_{i=2}^{3} \sum_{j=1}^{3} y_D^{ij} N_i^c L_j H_u + \sum_{k=1}^{3} y_k \Phi N_k^c N_k^c - \mu_\Phi \bar{\Phi} \Phi, \quad (1)$$

where the first term is the neutrino Dirac Yukawa coupling, the second term is the Majorana Yukawa coupling for the right-handed neutrinos, and a SUSY mass term for the SM singlet Higgs fields is given in the third term. Without loss of generality, we have worked in the basis where the Majorana Yukawa coupling matrix is real and diagonal.

---

[1]It is possible to construct a phenomenologically viable SUSY $B - L$ model without Φ and $\bar{\Phi}$ [13].

TABLE I. Particle contents: In addition to the MSSM particles, three right-handed neutrino superfields ($N^c_{1,2,3}$) and two Higgs superfields ($\bar{\Phi}$ and Φ) are introduced. The Z_2 parity for N^c_1 is assigned to be odd, and $i = 1, 2, 3$ is the generation index.

Chiral superfield	$SU(3)_c$	$SU(2)_L$	$U(1)_Y$	$U(1)_X$	R parity	Z_2
Q^i	**3**	**2**	$+1/6$	$(1/6)x_H + 1/3$	$-$	$+$
U^c_i	**3***	**1**	$-2/3$	$(-2/3)x_H - 1/3$	$-$	$+$
D^c_i	**3***	**1**	$+1/3$	$(1/3)x_H - 1/3$	$-$	$+$
L_i	**1**	**2**	$-1/2$	$(-1/2)x_H - 1$	$-$	$+$
N^c_1	**1**	**1**	0	$+1$	$-$	$-$
$N^c_{2,3}$	**1**	**1**	0	$+1$	$-$	$+$
E^c_i	**1**	**1**	$+1$	$x_H + 1$	$-$	$+$
H_u	**1**	**2**	$+1/2$	$(1/2)x_H$	$+$	$+$
H_d	**1**	**2**	$-1/2$	$(-1/2)x_H$	$+$	$+$
Φ	**1**	**1**	0	-2	$+$	$+$
$\bar{\Phi}$	**1**	**1**	0	$+2$	$+$	$+$

Note that Dirac Yukawa couplings between N^c_1 and L_j are forbidden by the Z_2 parity, so that the lightest component field in N^c_1 is stable, as long as the Z_2 parity is exact.

As we will discuss in the next section, the $U(1)_X$ gauge symmetry is radiatively broken at the TeV scale, and the right-handed neutrinos obtain TeV-scale Majorana masses. The seesaw mechanism[2] sets the mass scale of light neutrinos at $m_\nu = m^T_D M^{-1}_R m_D = \frac{v^2_u}{2} y^T_D M^{-1}_R y_D$, where v_u is the VEV of the up-type Higgs doublet in the MSSM, M_R is the 2×2 mass matrix of the right-handed neutrinos, and y_D is the 2×3 Dirac Yukawa coupling matrix from Eq. (1). It is natural to assume that the mass of the heaviest light neutrino is $m_\nu \sim \sqrt{\Delta m^2_{23}} \sim 0.05$ eV with $\Delta m^2_{23} \simeq 2.43 \times 10^{-3}$ eV^2 being the atmospheric neutrino oscillation data [1]. Thus, we estimate $y_D \sim 10^{-6}$ and point out that such a small neutrino Dirac Yukawa coupling is negligible in the analysis of RGEs.

Next, we introduce soft SUSY breaking terms for the fields in the $U(1)_X$ sector,

$$
\mathcal{L}_{\text{soft}} = -\left(\frac{1}{2}M_X \lambda_X \lambda_X + \text{H.c.}\right)
$$
$$
- \left(\sum_{k=1}^{3} m^2_{\tilde{N}^c_k}|\tilde{N}^c_k|^2 + m^2_\Phi|\Phi|^2 + m^2_{\bar\Phi}|\bar\Phi|^2\right)
$$
$$
+ \left(B_\Phi \bar\Phi\Phi + \sum_{k=1}^{3} A_k \Phi\tilde{N}^c_k\tilde{N}^c_k + \text{H.c.}\right). \quad (2)
$$

Here we have omitted terms relevant to the neutrino Dirac Yukawa couplings since they are very small, i.e., $\mathcal{O}(10^{-6})$

or smaller. For simplicity, in this analysis we consider the same setup as the constrained MSSM and assume the universal soft SUSY breaking parameters $m^2_{\tilde{N}^c_k} = m^2_\Phi = m^2_{\bar\Phi} = m^2_0$ and $A_k = A_0$ at the grand unification scale[3] $M_U = 2 \times 10^{16}$ GeV.

Before closing this section, we comment on the uniqueness of the Z_2-parity assignment from the phenomenological point of view. One may find the Z_2-parity assignment *ad hoc*, but we cannot assign an odd parity for any MSSM particles because the parity forbids the Dirac Yukawa couplings, which is necessary to reproduce the observed fermion masses and quark flavor mixings. As we will see in the next section, the scalars Φ and $\bar\Phi$ develop nonzero VEVs to break the $U(1)_X$ gauge symmetry, and these fields should be Z_2 parity even in order to generate the Majorana masses for the right-handed neutrinos. Hence, we can assign Z_2-odd parity only for right-handed neutrinos. Considering the fact that we need at least two right-handed neutrinos to reproduce the observed neutrino oscillation data, two right-handed neutrinos should be parity even and be involved in the seesaw mechanism. As a result, we have assigned Z_2 parity odd for only one right-handed neutrino, as in Table I. This Z_2 parity can be considered as an enhanced global symmetry, which becomes manifest after taking the Dirac Yukawa coupling of N^c_1 to zero.

III. RADIATIVE $U(1)_X$ SYMMETRY BREAKING AND R PARITY

In the non-SUSY minimal $U(1)_X$ model, the $U(1)_X$ symmetry breaking scale is determined by parameters in

---

[2]As we will see in the next section, R parity is also radiatively broken. In this case, the right-handed neutrinos mix with the $B - L$ gaugino and fermionic components of $\bar\Phi$ and Φ, and the seesaw formula is quite involved.

[3]However, we do not necessarily assume grand unification behind our model. In fact, it is very nontrivial to unify the Z_2-odd right-handed neutrino with Z_2-even fields.

the Higgs potential which can, in general, be at any scale as long as the experimental constraints are satisfied. The large electron positron (LEP) experiment has set the lower bound on the $B - L$ symmetry breaking scale as $m_{Z'}/g_{BL} \geq 6\text{--}7$ TeV [14]. The most recent LHC results for Z' boson search with 139 fb^{-1} [15] excluded the $B - L$ Z' gauge boson mass $m_{Z'} \lesssim 5.1$ TeV. We see that the LHC bound is more severe than the LEP bound. The SUSY extension of the model, however, offers a very interesting possibility for constraining the $B - L$ [and thereby $U(1)_X$] symmetry breaking scale, as pointed out in [8].

It is well known that the electroweak symmetry breaking in the MSSM is triggered by radiative corrections to the up-type Higgs doublet mass squared via the large top Yukawa coupling [16]. Directly analogous to this situation, the $U(1)_X$ symmetry breaking occurs through radiative corrections with a large Majorana Yukawa coupling.

We consider the following RGEs for soft SUSY breaking terms in the $U(1)_X$ sector [9,17]:

$$16\pi^2 \mu \frac{dM_X}{d\mu} = 2(24 + 16x_H + 11x_H^2)g_X^2 M_X,$$

$$16\pi^2 \mu \frac{dm_{\tilde{N}_i^c}^2}{d\mu} = 8y_i^2 m_\Phi^2 + 16y_i^2 m_{\tilde{N}_i^c}^2 + 8A_i^2 - 8g_X^2 M_X^2,$$

$$16\pi^2 \mu \frac{dm_\Phi^2}{d\mu} = 4\left(\sum_{i=1}^3 y_i^2\right)m_\Phi^2 + 8\sum_{i=1}^3 y_i^2 m_{\tilde{N}_i^c}^2$$
$$+ 4\sum_{i=1}^3 A_i^2 - 32g_X^2 M_X^2,$$

$$16\pi^2 \mu \frac{dm_{\bar{\Phi}}^2}{d\mu} = -32g_X^2 M_X^2,$$

$$16\pi^2 \mu \frac{dA_i}{d\mu} = \left(30y_i^2 + 2\sum_{j\neq i} y_j^2 - 12g_X^2\right)A_i$$
$$+ 4y_i\left(\sum_{j\neq i} y_j A_j - 6g_X^2 M_X\right), \quad (3)$$

where RGEs for the gauge and Yukawa couplings are given by

$$16\pi^2 \mu \frac{dg_X}{d\mu} = (24 + 16x_H + 11x_H^2)g_X^3,$$

$$16\pi^2 \mu \frac{dy_i}{d\mu} = y_i\left(10y_i^2 + 2\sum_{j\neq i} y_j^2 - 12g_X^2\right). \quad (4)$$

To illustrate the radiative $U(1)_X$ symmetry breaking, we solve these equations from $M_U = 2 \times 10^{16}$ GeV to low energy, choosing $x_H = -0.8$ and the following boundary conditions:
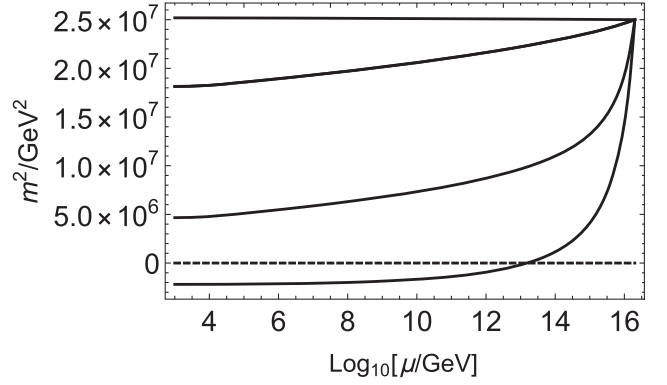

FIG. 1. The RGE running of the soft SUSY breaking masses, $m_{\bar{\Phi}}^2$ (top curve), $m_{\tilde{N}_1^c}^2 = m_{\tilde{N}_2^c}^2$ (second from the top), m_Φ^2 (third from the top), and $m_{\tilde{N}_3^c}^2$ (bottom curve) shown in Eq. (3).

$$g_X = 0.532, \quad y_1 = y_2 = 0.4, \quad y_3 = 2.5,$$
$$M_X = 1 \text{ TeV}, \quad m_{\tilde{N}_i^c} = m_\Phi = m_{\bar{\Phi}} = 5 \text{ TeV}, \quad A_i = 0. \quad (5)$$

The RGE running of soft SUSY breaking masses as a function of the renormalization scale is shown in Fig. 1. After the RGE running, $m_{\tilde{N}_3^c}^2$ becomes negative while the other squared masses remain positive. The negative mass squared of the right-handed sneutrino triggers not only the $U(1)_X$ symmetry breaking but also R-parity violation. Detailed analysis with random values of parameters has shown [9] that, in most of the parameter region realizing the radiative $B - L$ symmetry breaking, R parity is also broken.

We now analyze the scalar potential with the soft SUSY breaking parameters obtained from solving RGEs. Since the $U(1)_X$ symmetry breaking scale is set to be 26 TeV in the following, we evaluate the RGE solutions at 26 TeV as follows:

$$g_X = 0.192, \quad y_1 = y_2 = 0.264, \quad y_3 = 0.533,$$
$$M_X = 766 \text{ GeV}, \quad m_{\tilde{N}_1^c}^2 = m_{\tilde{N}_2^c}^2 = 1.83 \times 10^7 \text{ GeV}^2,$$
$$m_{\tilde{N}_3^c}^2 = -2.18 \times 10^6 \text{ GeV}^2,$$
$$m_\Phi^2 = 4.91 \times 10^6 \text{ GeV}^2, \quad m_{\bar{\Phi}}^2 = 2.52 \times 10^7 \text{ GeV}^2,$$
$$A_1 = A_2 = 30.4 \text{ GeV}, \quad A_3 = 36.5 \text{ GeV}. \quad (6)$$

The scalar potential for $\tilde{N}_3^c$, Φ, and $\bar{\Phi}$ consists of supersymmetric terms and soft SUSY breaking terms,

$$V = V_{\text{SUSY}} + V_{\text{Soft}}, \quad (7)$$

where

$$V_{\text{SUSY}} = |2y_3\tilde{N}_3^c\Phi|^2 + |\mu_\Phi\Phi|^2 + |y_3(\tilde{N}_3^c)^2 - \mu_\Phi\bar{\Phi}|^2$$
$$+ \frac{g_X^2}{2}(|\tilde{N}_3^c|^2 - 2|\Phi|^2 + 2|\bar{\Phi}|^2)^2,$$
$$V_{\text{Soft}} = m_{\tilde{N}_3^c}^2|\tilde{N}_3^c|^2 + m_\Phi^2|\Phi|^2 + m_{\bar{\Phi}}^2|\bar{\Phi}|^2$$
$$- (A_3\Phi\tilde{N}_3^c\tilde{N}_3^c + B_\Phi\bar{\Phi}\Phi + \text{H.c.}). \tag{8}$$

With appropriate values of μ_Φ and B_Φ, stationary conditions for the scalar potential can be found numerically. For example, we find (in units of TeV)

$$\langle\tilde{N}_3^c\rangle = \frac{12.5}{\sqrt{2}}, \qquad \langle\Phi\rangle = \frac{6.56}{\sqrt{2}}, \qquad \langle\bar{\Phi}\rangle = \frac{9.29}{\sqrt{2}} \tag{9}$$

for $\mu_\Phi = 6.96$ TeV, $B_\Phi = 66.0$ TeV^2, and the parameters given in Eq. (6). In this case, we have the Z' boson mass

$$m_{Z'} = g_X v_X = 5 \text{ TeV}, \tag{10}$$

where

$$v_X = \sqrt{2\langle\tilde{N}_3^c\rangle^2 + 8\langle\Phi\rangle^2 + 8\langle\bar{\Phi}\rangle^2} = 26 \text{ TeV} \tag{11}$$

and the experimental lower bound $v_{BL} \geq 6$–7 TeV [14] is satisfied.

In order to prove that the stationary point is actually the potential minimum, we calculate the mass spectrum of the scalars, $\tilde{N}_3^c$, Φ, and $\bar{\Phi}$. By straightforward numerical calculations, we find the eigenvalues of the mass matrix of the scalars $\Re[\tilde{N}_3^c]$, $\Re[\Phi]$, and $\Re[\bar{\Phi}]$ as (13.7,4.34,4.75) in TeV and the mass eigenvalues for the pseudoscalars $\Im[\tilde{N}_3^c]$, $\Im[\Phi]$, and $\Im[\bar{\Phi}]$ as (0,8.82,12.8) in TeV. As expected, there is one massless eigenstate corresponding to the would-be Nambu-Goldstone mode. The other right-handed sneutrino mass eigenvalues are given by

$$m_{\tilde{N}_{Ri}}^2 = m_{\tilde{N}_i^c}^2 + 4y_i^2\langle\Phi\rangle^2 - 2y_iy_3\langle\tilde{N}_3^c\rangle^2 + 2A_i\langle\Phi\rangle$$
$$+ 2y_i\mu_\Phi\langle\bar{\Phi}\rangle + D_X,$$
$$m_{\tilde{N}_{Ii}}^2 = m_{\tilde{N}_i^c}^2 + 4y_i^2\langle\Phi\rangle^2 + 2y_iy_3\langle\tilde{N}_3^c\rangle^2 - 2A_i\langle\Phi\rangle$$
$$- 2y_i\mu_\Phi\langle\bar{\Phi}\rangle + D_X, \tag{12}$$

where $m_{\tilde{N}_{Ri}}$ and $m_{\tilde{N}_{Ii}}$ ($i = 1, 2$) are the mass eigenvalues for scalars and pseudoscalars, respectively, and $D_X = g_X^2(\langle\tilde{N}_3^c\rangle^2 - 2\langle\Phi\rangle^2 + 2\langle\bar{\Phi}\rangle^2)$. We find $m_{\tilde{N}_{R1}} = m_{\tilde{N}_{R2}} = 5.58$ and $m_{\tilde{N}_{I1}} = m_{\tilde{N}_{I2}} = 5.16$ TeV. Since the fermion components in $N_{2,3}^c$, Φ, and $\bar{\Phi}$ and the $U(1)_X$ gauginos are all mixed, it is quite involved to find the Majorana fermion mass eigenvalues. Accordingly, the seesaw mechanism is realized in a very complicated way. Although we do not discuss the fermion spectrum in detail here, our system

with two right-handed neutrinos coupling to the SM neutrinos provides many free parameters; enough to reproduce the observed neutrino oscillation data. On the other hand, the mass of the Z_2-odd right-handed neutrino N_1^c is simply given by[4]

$$M_{N_1^c} = 2y_1\langle\Phi\rangle = 2.45 \text{ TeV} \simeq m_{Z'}/2. \tag{13}$$

IV. RIGHT-HANDED NEUTRINO DARK MATTER

As we showed in the previous section, the $U(1)_X$ gauge symmetry is radiatively broken at the TeV scale. Associated with this radiative breaking, the right-handed sneutrino $\tilde{N}_3^c$ develops VEV and, as a result, R parity is also broken. Therefore, the neutralino is no longer the dark matter candidate. However, note that in our model the Z_2 parity is still exact, by which the lightest Z_2-odd particle is stable and can play the role of dark matter even in the presence of R-parity violation. As is evident in the mass spectrum we found in the previous section, the right-handed neutrino N_1^c is the lightest Z_2-odd particle. In this section, we evaluate the relic abundance of this right-handed neutrino dark matter candidate and identify the parameter region(s) consistent with the observations.

In [11], the relic abundance of the right-handed neutrino dark matter is analyzed in detail, where annihilation processes through the SM Higgs boson in the s channel play the crucial role to reproduce the observed dark matter relic abundance. In the non-SUSY minimal $B - L$ model, the right-handed neutrino can have a sizable coupling with the SM Higgs boson due to the mixing between the SM Higgs doublet and the $B - L$ Higgs in the scalar potential. However, in supersymmetric extension of the $U(1)_X$ model, there is no mixing between the MSSM Higgs doublets and the $U(1)_X$ Higgs superfields in the starting superpotential. Although such a mixing emerges through the neutrino Dirac Yukawa coupling with the VEV of the right-handed sneutrino $\tilde{N}_3^c$, it is very small because of the small neutrino Dirac Yukawa coupling $y_D = \mathcal{O}(10^{-6})$. Among several annihilation channels of a pair of the Z_2-odd right-handed neutrinos, we find that the s-channel Z' boson exchange process gives the dominant contribution.

Now we evaluate the relic abundance of the right-handed neutrino by integrating the Boltzmann equation [18],

$$\frac{dY_{N_1^c}}{dx} = -\frac{x\gamma_{Z'}}{sH(M)}\left[\left(\frac{Y_{N_1^c}}{Y_{N_1^c}^{eq}}\right)^2 - 1\right], \tag{14}$$

---

[4]It is generally possible to have a sneutrino dark matter (DM) candidate, however, due to the LHC bound on the Z' gauge coupling, the corresponding VEV must be large. It would be difficult to tune the sneutrino mass to be half the Z' mass in order to achieve the correct relic abundance constraint discussed in Sec. IV.

where $Y_{N_1^c}$ is the yield (the ratio of the number density to the entropy density s) of the Z_2-odd right-handed neutrino, $Y_{N_1^c}^{eq}$ is the yield in thermal equilibrium, the temperature of the Universe is normalized by the mass of the right-handed neutrino $x = M/T$, and $H(M)$ is the Hubble parameter at $T = M$. The space-time densities of the scatterings mediated by the s-channel Z' boson exchange in thermal equilibrium are given by

$$\gamma_{Z'} = \frac{T}{64\pi^4} \int_{4M^2}^{\infty} ds\hat{\sigma}(s)\sqrt{s}K_1\left(\frac{\sqrt{s}}{T}\right), \quad (15)$$

where s is the squared center-of-mass energy, K_1 is the modified Bessel function of the first kind, and the total reduced cross section for the process $N_1^c N_1^c \to Z' \to f\bar{f}$ (f denotes the SM fermions) is

$$\hat{\sigma}_{Z'}(s) = \frac{1}{24\pi} g_X^4 \frac{\sqrt{s}(s-4M^2)^{\frac{3}{2}}}{(s-m_{Z'}^2)^2 + m_{Z'}^2\Gamma_{Z'}^2} F(x_H), \quad (16)$$

with the decay width of the Z' boson,

$$\Gamma_{Z'} = \frac{g_X^2}{24\pi}\left[F(x_H) + 2\left(1-\frac{4M^2}{m_{Z'}^2}\right)^{\frac{3}{2}}\theta(m_{Z'}^2/M^2 - 4)\right], \quad (17)$$

where

$$F(x_H) = (13 + 16x_H + 10x_H^2). \quad (18)$$

For simplicity, we have assumed that $y_1 = y_2$ as in the previous section and that the other particles (except for the SM particles) are all heavy with mass $> m_{Z'}/2$. This assumption is consistent with the parameter choice in our analysis below.

Now we solve the Boltzmann equation numerically. To solve the equation for the relevant domain, we inherit parameter values from those presented in the previous section which were already motivated as interesting values,

$$g_X = 0.192, \qquad m_{Z'} = 5 \text{ TeV}, \quad (19)$$

while $M_{N_1^c} = M$ is taken to be a free parameter. With the asymptotic value of the yield $Y_{N_1^c}(\infty)$, the dark matter relic density is written as

$$\Omega h^2 = \frac{M s_0 Y_{N_1^c}(\infty)}{\rho_c/h^2}, \quad (20)$$

where $s_0 = 2890 \text{ cm}^{-3}$ is the entropy density of the present Universe, and $\rho_c/h^2 = 1.05 \times 10^{-5} \text{ GeV/cm}^3$ is the critical density. The result should be compared with the observations at 2σ level [19],

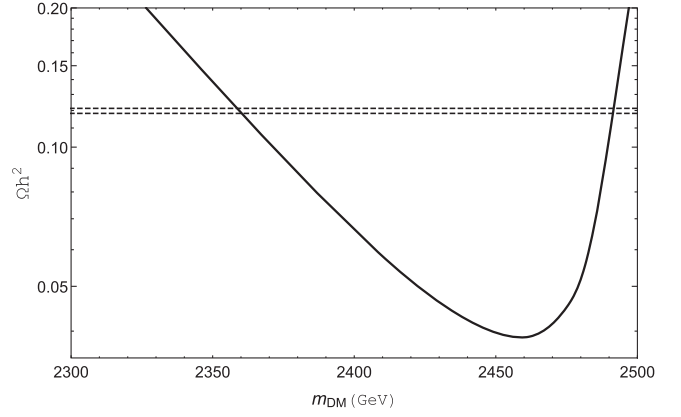$$\Omega_{\text{DM}}h^2 = 0.1198 \pm 0.0015. \quad (21)$$

FIG. 2. The relic abundance of the dark matter right-handed neutrino as a function of its mass for the $U(1)_X$ ($x_H = -0.8$) scenario. The dashed lines represent the upper and the lower bounds on the dark matter relic abundance, $0.1183 \le \Omega_{\text{DM}}h^2 \le 0.1213$.

Figure 2 shows the relic abundance of the right-handed neutrino dark matter as a function of its mass. The dashed lines correspond to the upper and the lower bounds on the dark matter relic abundance in Eq. (21). We find two solutions,

$$M \simeq 2359, \quad 2492 \text{ GeV}. \quad (22)$$

It turns out from Fig. 2 that, in order to reproduce the observed relic abundance, the enhancement of the annihilation cross section is necessary so that the mass of the dark matter should be close to the Z' boson resonance point.[5] The dark matter mass $M = 2492$ GeV coincides with the value presented in the previous section. For a different parameter choice, the Z_2-odd right-handed sneutrino [the lighter of its scalar (S) or pseudoscalar (P) components] can be the lightest Z_2-odd particle and a candidate for the dark matter, instead of the right-handed neutrino. In this case, the main dark matter annihilation process is the coannihilation process, $SP \to Z'$. Note that Eq. (12) indicates a sizable mass splitting between S and P. This means that the coannihilation process is not efficient even with the Z' resonance effect, since the number density of the particle that the dark matter particle coannihilates with is suppressed much more than the dark matter number density.

The RHN DM can scatter off with nuclei via Z' boson exchange. Since the RHN DM is a Majorana particle, only its interaction with nuclei is spin dependent in the non-relativistic limit. We have estimated this spin-dependent cross section to be $\sigma_{\text{SD}} \sim 10^{-9}$ pb, which is far below

_____

[5]As the Z' boson partial decay width to a DM pair is negligibly small, the associated branching ratio is tiny [$\mathcal{O}(0.1\%)$]. At this stage, it is very challenging to understand the right-handed neutrino (RHN) DM existence directly through the Z' boson measurement, but a future lepton collider such as the muon collider might be able to test our scenario with its TeV-scale collider energy and high precision measurements.
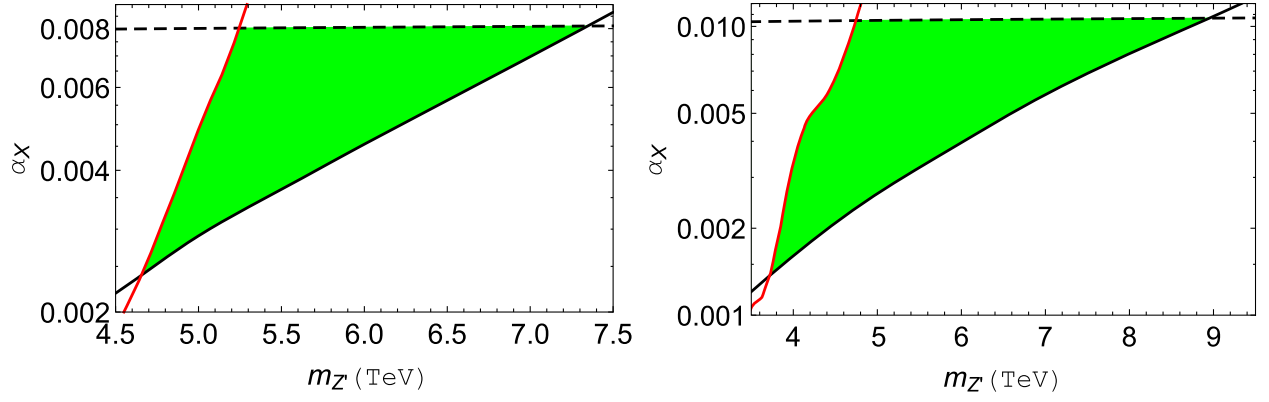
FIG. 3. Combining the perturbativity constraints from solving the RGEs given by the dashed horizontal line (in black) and the DM relic abundance constraints, previously discussed and shown by the lower solid curve (in black), yields a narrow allowed parameter region (shaded green) for the $U(1)_X$ model in the $B - L$ [$SU(5)$] scenario, $x_H = 0$ ($x_H = -0.8$) on the left (right). The diagonal solid line (in red) shows the updated LHC results. The LEP results are much less confining and well outside the confining region.

the current upper bounds, $\sigma_{SD} \sim 10^{-5}$ pb for $m_{DM} = \mathcal{O}(1 \text{ TeV})$ [20].

V. LHC CONSTRAINTS AND COMPLEMENTARITY WITH COSMOLOGICAL BOUNDS

The differential cross section for the process, $pp \to Z' + X \to \ell^+\ell^- + X; \ell^+\ell^- = e^+e^-/\mu^+\mu^-$, with respect to the dilepton invariant mass $M_{\ell\ell}$ is given by

$$\frac{d\sigma}{dM_{\ell\ell}} = \sum_{q,\bar{q}} \int_{\frac{M^2_{\ell\ell}}{E^2_{LHC}}}^{1} dx \frac{2M_{\ell\ell}}{xE^2_{LHC}} f_q(x,Q^2) f_{\bar{q}}\left(\frac{M^2_{\ell\ell}}{xE^2_{LHC}}, Q^2\right)$$
$$\times \hat{\sigma}(q\bar{q} \to Z' \to \ell^+\ell^-), \tag{23}$$

where Q is the factorization scale (we fix $Q = m_{Z'}$, for simplicity), $E_{LHC} = 13$ TeV is the center-of-mass energy of the LHC run 2, f_q ($f_{\bar{q}}$) is the parton distribution function for quark (antiquark), and the cross section for the colliding partons is described as

$$\hat{\sigma}(q\bar{q} \to Z' \to \ell^+\ell^-) = \frac{\pi}{1296} \alpha_X^2 \frac{M^2_{\ell\ell}}{(M^2_{\ell\ell} - m^2_{Z'})^2 + m^2_{Z'}\Gamma^2_{Z'}}$$
$$\times F_{q\ell}(x_H), \tag{24}$$

where the function $F_{q\ell}(x_H)$ is given by

$$F_{u\ell}(x_H) = (8 + 20x_H + 17x_H^2)(8 + 12x_H + 5x_H^2),$$
$$F_{d\ell}(x_H) = (8 - 4x_H + 5x_H^2)(8 + 12x_H + 5x_H^2), \tag{25}$$

with q being the up-type (u) and down-type (d) quarks, respectively. In our analysis, we employ CTEQ6L [21] for the parton distribution functions and numerically evaluate the cross section of the dilepton production through the s-channel Z' boson exchange. Since the right-handed

neutrino DM mass must be close to half of the Z' boson mass, its contribution to the Z' boson decay width is negligibly small, and thus the resultant cross section is controlled by only three free parameters, α_X, $m_{Z'}$, and x_H. In interpreting the latest ATLAS results [22] for the upper bound on the cross section of the process $pp \to Z' + X \to \ell^+\ell^- + X$, we follow the strategy in Refs. [23–25]: we first calculate the cross section of the process by Eq. (23) and then we scale our cross section result to find a k factor ($k = 1.31$) by which our cross section coincides with the SM prediction of the cross section presented in the ATLAS paper [22]. This k factor is employed for all of our analysis. In this way, we find an upper bound on α_X as a function of $m_{Z'}$ (x_H) for a fixed value of x_H ($m_{Z'}$).

The LEP experiments have searched for effective four Fermi interactions mediated by a Z' boson [26] and no significant deviation from the SM predictions have been observed. The LEP results are interpreted into a lower bound on $m_{Z'}/\sqrt{\alpha_X}$ for a fixed x_H value, which means an upper bound on α_X as a function of $m_{Z'}$ for a fixed x_H value similar to the constraints obtained from the LHC run 2 results. For the minimal $U(1)_X$ model, the LEP bound on $m_{Z'}/\sqrt{\alpha_X}$ has been obtained in Refs. [24,27]. Since the $U(1)_X$ charge assignment for the SM fermions in our model is the same as in the minimal model, the LEP bound presented in Refs. [24,27] can be applied also to our model. Thus, we simply refer to the bound. We will see that the LHC constraints are much more severe than the LEP one for $m_{Z'} \lesssim 5$ TeV.

To constrain the model parameter space further, we may also consider a theoretical upper bound on α_X, namely, the perturbativity bound on the gauge coupling. Recall that the β function coefficient of the RGE for the $U(1)_X$ gauge coupling from Eq. (4) and the particle contents from Table I is given by

$$b_X = 24 + 16x_H + 11x_H^2, \tag{26}$$

which is large compared to the SM $U(1)_Y$ RGE coefficient. To keep the running $U(1)_X$ gauge coupling $\alpha_X(\mu)$ in the perturbative regime up to the Planck scale ($M_{\rm Pl} = 1.22 \times 10^{19}$ GeV), an upper bound on α_X at low energies can be derived. Solving the RG equation for the $U(1)_X$ gauge coupling at the one-loop level, we find the relation between the gauge coupling at $m_{Z'}$ (denoted as α_X in our DM and LHC analysis) and the one at the Planck scale $\alpha_X(M_{\rm Pl})$,

$$\alpha_X = \frac{\alpha_X(M_{\rm Pl})}{1 + \alpha_X(M_{\rm Pl}) \frac{b_X}{2\pi} \ln\left[\frac{M_{\rm Pl}}{m_{Z'}}\right]}. \qquad (27)$$

For simplicity, we have set a common mass for all new particles to be $m_{Z'}$. Effects of mass splittings are negligibly small unless the new particle mass spectrum is hierarchical. Imposing the perturbativity bound of $\alpha_X(M_{\rm Pl}) \leq 4\pi$, we find an upper bound on α_X for the fixed values of $m_{Z'}$ and x_H.

Let us now combine all constraints. We have obtained the lower bound on α_X from the observed DM relic abundance. On the other hand, the upper bound on α_X has been obtained from the LHC results from the search for a narrow resonance, the LEP results, and the coupling perturbativity up to the Planck scale. Note that these constraints are complementary to narrow down the model parameter space.[6] In Fig. 3, we show the combined results for $x_H = 0$ ($x_H = -0.8$) in the left (right) panel. The (black) solid lines are the cosmological lower bounds on α_X as a function of $m_{Z'}$. The red solid line is the upper bound on α_X from the LHC run 2 results. The perturbativity bounds on α_X are depicted by the black dashed lines. The regions satisfying all the constraints are green shaded.

Another interesting set of constraints on α_X to consider is found from combining a scan over x_H values for the DM relic abundance bound, the perturbativity bound, and the latest LHC bounds. We show our combined results in Fig. 4 for $m_{Z'} = 5$ TeV, where the red dashed and black solid curves represent the LHC and DM relic abundance bounds, respectively, and the black dashed curve illustrates the perturbativity bound on α_X. The green-shaded region is allowed after combining all the bounds. The LHC bound shows the peak at $x_H \sim -1$. This is because the functions $F_{u\ell}$ and $F_{d\ell}$ in Eq. (25) have the minimum at $x_H \sim -1$. Similarly, the perturbative bound shows the peak at $x_H \sim -0.7$ since the β function coefficient of Eq. (26) has the minimum at $x_H \sim -0.7$. As expected, the LHC bound becomes weaker as we increase $m_{Z'}$, leading to a wider green-shaded region. One can see from Fig. 4 that well within the allowed region (shaded green) sits the value of $x_H = -0.8$, which corresponds to the $SU(5)$ scenario discussed below. The fact that the $x_H = -0.8$ value lies in this region suggests that the $SU(5)$ scenario remains a
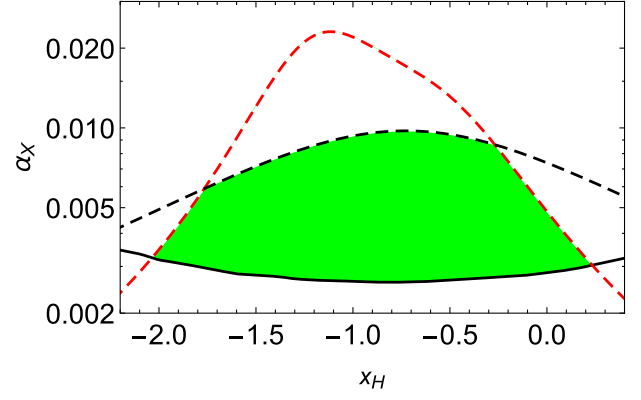

FIG. 4. A scan over x_H values for $m_{Z'} = 5$ TeV combines the DM relic abundance constraints shown by the solid lower curve (in black), the perturbativity constraints shown by the second dashed curve from the top (in black), and the LHC data with 139 fb^{-1} luminosity by the dashed upper curve (in red) [15]. This narrow region between the constraints (green shaded) show the allowed values for α_X. The value of $x_H = -0.8$ corresponds to the $SU(5)$ scenario and is seen to be well within this allowed parameter region.

viable description of nature, and as the LHC results are continually updated it will be interesting to see if the data continue to support the elegant $SU(5)$ case.

VI. $SU(5) \times U(1)_X$ GRAND UNIFIED THEORY (GUT) SCENARIO

Our setup can be readily extended to the $SU(5) \times U(1)_X$ gauge group. As has been previously shown in the non-SUSY $SU(5) \times U(1)_X$ setup in Ref. [28], this corresponds to the scenario where $x_H = -0.8$. Only with this choice for x_H can the quarks and leptons be unified into the same super-multiplet, where the MSSM chiral superfields are arranged into the three generations of **10** and **5*** representations under $SU(5)$. The H_u and H_d superfields are in the **5** and **5*** representations, respectively. The N_k^c, Φ, and $\bar{\Phi}$ superfields are all singlets under $SU(5)$. An additional superfield that is neutral under $U(1)_X$ and in the **24** representation of $SU(5)$ is required in order to break $SU(5) \times U(1)_X$ down to $SU(3)_C \times SU(2)_L \times U(1)_Y \times U(1)_X$. We consider the same $SU(5)$ breaking paradigm for the **24** considered in [29], and we find that the unification scale for the SM gauge couplings occurs at $M_{\rm GUT} \simeq 2 \times 10^{16}$ GeV. After $SU(5)$ has been broken down to the SM gauge groups at $M_{\rm GUT}$, a kinetic mixing between the $U(1)_Y$ and $U(1)_X$ gauge fields occurs due to the evolution of the RGEs.

Following the procedure outlined in Ref. [28], the basis is chosen such that the gauge boson kinetic terms are all diagonalized. The covariant derivative of a field is given by

---

[6]We see that the LEP bound is always much weaker than the LHC bounds (for $m_{Z'} \leq 5$ TeV) and the perturbativity bound. We have considered the LEP bound for completeness.

$$D_\mu = \partial_\mu - (Y \quad Q_X) \begin{pmatrix} g_1 & g_{\rm mix} \\ 0 & g_X \end{pmatrix} \begin{pmatrix} B_\mu \\ Z'_\mu \end{pmatrix}, \qquad (28)$$

where the Y and Q_X are the $U(1)_Y$ and $U(1)_X$ field charges, respectively, B_μ and Z'_μ are the SM $U(1)_Y$ and $U(1)_X$ gauge fields, and $g_1 = \sqrt{5/3}g_Y$ and g_X are the $U(1)_Y$ and $U(1)_X$ gauge couplings. As a result of the original gauge kinetic mixing, a new parameter dubbed the "mixed gauge coupling" is introduced. In this chosen basis, the RGE evolution of the SM g_1 gauge coupling remains unaffected, whereas the g_X and $g_{\rm mix}$ evolution evolve according to their coupled RGEs. At one-loop level, the RGEs for $\mu > \mathcal{O}(\text{TeV})$ are given by

$$16\pi^2\mu\frac{dg_X}{d\mu} = g_X((24 + 16x_H + 11x_H^2)g_X^2$$
$$+ 2(8 + 11x_H)g_X g_{\rm mix} + 11g_{\rm mix}^2),$$
$$16\pi^2\mu\frac{dg_{\rm mix}}{d\mu} = g_{\rm mix}((24 + 16x_H + 11x_H^2)g_X^2$$
$$+ 2(8 + 11x_H)g_X g_{\rm mix} + 11g_{\rm mix}^2)$$
$$+ \frac{6}{5}g_1^2((8 + 11x_H)g_X + 11g_{\rm mix}). \tag{29}$$

These RGEs encompass the effects of all particles in the theory present at the TeV scale. The RGEs in Eq. (29) have been solved numerically with $g_{\rm mix} = 0$ and various values of g_X at $\mu = M_{\rm GUT}$. Regardless of the boundary value of g_X at $M_{\rm GUT}$, we have found that the ratio is always $g_{\rm mix}/g_X \simeq 0.042$ at the TeV scale. The fact that this ratio is so small means that we can safely make the approximation to neglect the mixed gauge coupling in our analysis and set $g_{\rm mix} = 0$. This approximation is consistent with all of our previous results attained for the $x_H = -0.8$ scenario.

VII. CONCLUSIONS AND DISCUSSIONS

The minimal gauged $U(1)_X$ model based on the gauge group $SU(3)_c \times SU(2)_L \times U(1)_Y \times U(1)_X$ is an elegant and simple extension of the Standard Model, in which the right-handed neutrinos of three generations are necessarily introduced for the gauge and gravitational anomaly cancellations. The mass of right-handed neutrinos arises associated with the $U(1)_X$ gauge symmetry breaking, and the seesaw mechanism is naturally implemented. The supersymmetric extension of the minimal $U(1)_X$ model offers not only a solution to the gauge hierarchy problem but also a natural mechanism of breaking the $U(1)_X$ symmetry at the TeV scale through the radiative $U(1)_X$ symmetry breaking. Although the radiative symmetry breaking at the TeV scale is a remarkable feature of the model, R parity is also broken by nonzero VEV of a right-handed sneutrino. Therefore, the neutralino, which is the conventional dark matter candidate in SUSY models, becomes unstable and cannot play the role of the dark matter any more.

We have proposed the use of a Z_2 parity and assigned an odd parity to one right-handed neutrino. This parity ensures the stability of the right-handed neutrino and hence the right-handed neutrino can remain a viable dark matter candidate even in the presence of R-parity violation. In this way, no new particles need to be introduced as a candidate for dark matter. We have shown that, for a parameter set, the mass squared of a right-handed sneutrino is driven to be negative by the RGE running. Analyzing the scalar potential with RGE solutions of soft SUSY breaking parameters, we have identified the vacuum where the $U(1)_X$ symmetry as well as R parity is broken at the TeV scale.

We have numerically integrated the Boltzmann equation for the Z_2-odd right-handed neutrino and found that its relic abundance is consistent with the observations. In reproducing the observed dark matter relic density, an enhancement of the annihilation cross section via the Z' boson s-channel resonance is necessary, so that the dark matter mass should be close to half of the Z' boson mass.

Associated with the $U(1)_X$ symmetry breaking, all new particles have TeV-scale masses, which is being tested at the LHC in operation. Discovery of the Z' boson resonance at the LHC [30] is the first step to confirm our model. Once the Z' boson mass is measured, the dark matter mass is also determined in our model. If kinematically allowed, the Z' boson decays to the dark matter particles with the branching ratio $\sim 0.3\%$ [see Eq. (17)]. Precise measurement of the invisible decay width of the Z' boson can reveal the existence of the dark matter particle.

We have also shown that the $SU(5) \times U(1)_X$ GUT scenario remains a possible description of nature by combining the constraints on the α_X coupling from the perturbativity bound LHC results on the process $pp \to Z' + X \to \ell^+\ell^- + X; \ell^+\ell^- = e^+e^-/\mu^+\mu^-$ and DM relic abundance bound seen in Fig. 3. As seen in this figure, the lower mass bound for the Z' boson is around 5 TeV for this scenario. By scanning over x_H values, one can see in Fig. 4 that the $x_H = -0.8$ value corresponding to $SU(5)$ remains in the narrow region of viability.

[1] K. Nakamura *et al.* (Particle Data Group Collaboration), J. Phys. G **37**, 075021 (2010).

[2] P. Minkowski, Phys. Lett. **67B**, 421 (1977); T. Yanagida, in *Proceedings of the Workshop on the Unified Theory and the Baryon Number in the Universe*, edited by O. Sawada and A. Sugamoto (KEK, Tsukuba, Japan, 1979), p. 95; M. Gell-Mann, P. Ramond, and R. Slansky, *Supergravity*, edited by P. van Nieuwenhuizen *et al.* (North Holland, Amsterdam, 1979), p. 315; S. L. Glashow, The future of elementary particle physics, in *Proceedings of the 1979 Cargèse Summer Institute on Quarks and Leptons*, edited by M. Lévy *et al.* (Plenum Press, New York, 1980), p. 687; R. N. Mohapatra and G. Senjanović, Phys. Rev. Lett. **44**, 912 (1980).

[3] R. N. Mohapatra and R. E. Marshak, Phys. Rev. Lett. **44**, 1316 (1980); R. E. Marshak and R. N. Mohapatra, Phys. Lett. **91B**, 222 (1980); C. Wetterich, Nucl. Phys. **B187**, 343 (1981); A. Masiero, J. F. Nieves, and T. Yanagida, Phys. Lett. **116B**, 11 (1982); R. N. Mohapatra and G. Senjanovic, Phys. Rev. D **27**, 254 (1983); W. Buchmuller, C. Greub, and P. Minkowski, Phys. Lett. B **267**, 395 (1991).

[4] A. Das, N. Okada, and D. Raut, Phys. Rev. D **97**, 115023 (2018).

[5] A. Das, N. Okada, and D. Raut, Eur. Phys. J. C **78**, 696 (2018).

[6] S. Oda, N. Okada, and D. s. Takahashi, Phys. Rev. D **92**, 015026 (2015).

[7] See, for example, W. Emam and S. Khalil, Eur. Phys. J. C **55**, 625 (2007); K. Huitu, S. Khalil, H. Okada, and S. K. Rai, Phys. Rev. Lett. **101**, 181802 (2008); L. Basso, A. Belyaev, S. Moretti, and C. H. Shepherd-Themistocleous, Phys. Rev. D **80**, 055030 (2009); P. Fileviez Perez, T. Han, and T. Li, Phys. Rev. D **80**, 073015 (2009); L. Basso, A. Belyaev, S. Moretti, G. M. Pruna, and C. H. Shepherd-Themistocleous, Eur. Phys. J. C **71**, 1613 (2011).

[8] S. Khalil and A. Masiero, Phys. Lett. B **665**, 374 (2008).

[9] P. Fileviez Perez and S. Spinner, Phys. Rev. D **83**, 035004 (2011).

[10] F. Takayama and M. Yamaguchi, Phys. Lett. B **485**, 388 (2000); W. Buchmuller, L. Covi, K. Hamaguchi, A. Ibarra, and T. Yanagida, J. High Energy Phys. 03 (2007) 037.

[11] N. Okada and O. Seto, Phys. Rev. D **82**, 023507 (2010).

[12] Z. M. Burell and N. Okada, Phys. Rev. D **85**, 055011 (2012).

[13] V. Barger, P. Fileviez Perez, and S. Spinner, Phys. Rev. Lett. **102**, 181802 (2009).

[14] M. S. Carena, A. Daleo, B. A. Dobrescu, and T. M. P. Tait, Phys. Rev. D **70**, 093009 (2004); G. Cacciapaglia, C. Csaki, G. Marandella, and A. Strumia, Phys. Rev. D **74**, 033011 (2006).

[15] ATLAS Collaboration, Search for high-mass dilepton resonances using 139 fb^{-1} of pp collisions at $\sqrt{s} = 13$ TeV with the ATLAS detector, http://cds.cern.ch/record/2663393.

[16] L. E. Ibanez and G. G. Ross, Phys. Lett. **110B**, 215 (1982); K. Inoue, A. Kakuto, H. Komatsu, and S. Takeshita, Prog. Theor. Phys. **68**, 927 (1982); L. Alvarez-Gaume, M. Claudson, and M. B. Wise, Nucl. Phys. **B207**, 96 (1982); J. R. Ellis, J. S. Hagelin, D. V. Nanopoulos, and K. Tamvakis, Phys. Lett. **125B**, 275 (1983).

[17] R. J. Hernandez-Pinto and A. Perez-Lorenzana, arXiv: 1105.0713.

[18] See, for example, E. W. Kolb and M. S. Turner, *The Early Universe* (Addison-Wesley, Reading, MA, 1990).

[19] D. Larson, J. Dunkley, G. Hinshaw, E. Komatsu, M. R. Nolta, C. L. Bennett, B. Gold, M. Halpern *et al.*, Astrophys. J. Suppl. Ser. **192**, 16 (2011).

[20] J. Aalbers *et al.* (LZ Collaboration), Phys. Rev. Lett. **131**, 041002 (2023).

[21] J. Pumplin, D. R. Stump, J. Huston, H. L. Lai, P. M. Nadolsky, and W. K. Tung, J. High Energy Phys. 07 (2002) 012.

[22] M. Aaboud *et al.* (ATLAS Collaboration), J. High Energy Phys. 10 (2017) 182.

[23] N. Okada and S. Okada, Phys. Rev. D **93**, 075003 (2016).

[24] N. Okada and S. Okada, Phys. Rev. D **95**, 035025 (2017).

[25] For a review, see S. Okada, Adv. High Energy Phys. **2018**, 5340935 (2018).

[26] LEP and ALEPH and DELPHI and L3 and OPAL Collaborations and LEP Electroweak Working Group and SLD Electroweak Group and SLD Heavy Flavor Group Collaborations, arXiv:hep-ex/0312023; S. Schael *et al.* (ALEPH and DELPHI and L3 and OPAL and LEP Electroweak Collaborations), Phys. Rep. **532**, 119 (2013).

[27] A. Das, S. Oda, N. Okada, and D. s. Takahashi, Phys. Rev. D **93**, 115038 (2016).

[28] N. Okada, S. Okada, and D. Raut, Phys. Lett. B **780**, 422 (2018).

[29] S. Dimopoulos and H. Georgi, Nucl. Phys. **B193**, 150 (1981).

[30] For an analysis for Z' boson for a variety of models, see, for example, J. Erler, P. Langacker, S. Munir, and E. Rojas, J. High Energy Phys. 11 (2011) 076.